MÁSTER UNIVERSITARIO EN QUÍMICA ORGÁNICA

TRABAJO FIN DE MÁSTER

CURSO 2024-2025

Photocatalytic Cascade Cyclization using Isobutane: Unveiling a Regioselective Disparity

Nicolás Martínez Acevedo

Director/a/es: Martín Fañanás Mastral, Akshay Murali Nair

Lugar de realización: CiQUS, Santiago de Compostela

Julio, 2025

Index

1. Introduction 5
1.1. Photocatalytic Functionalization of Gaseous Alkanes 5
1.2. Radical Cascade Cyclization 8
2. Objective 10
3. Results and Discussion 11
3.1. Optimization of the reaction 11
3.2. Scope of the Reaction 13
3.3. Derivatization Product 14
3.4. Mechanistic Studies 15
4. Conclusions 17
5. References 17
6. Annex 20
6.1. General Experimental Details 20
6.2. General Procedures 21
6.3. Characterization of the Products 24
6.4. NMR Spectra of the Products (7-13) 28

Abbreviations and symbols

BDE	Bond dissociation energy
DCM	Dichloromethane
HAT	Hydrogen atom transfer
NFSI	*N*-fluorobenzenesulfonimide
HOMO	Highest occupied molecular orbital
LMCT	Ligand to metal charge transfer
LUMO	Lowest unoccupied molecular orbital
PFTB	Perfluoro-*tert*-butanol
PC	Photocatalyst
TEMPO	2,2,6,6-tetramethylpiperidin-1-oxyl
HAT	Hydrogen atom transfer
r.r.	Regioisomeric ratio
rt	Room temperature
SET	Single electron transfer
TBADT	Tetrabutylammonium decatungstate

Abstract

In this work, we present a novel photocatalytic hydrogen atom transfer (HAT)-based cascade cyclization of *N*-aryl acrylamides with isobutane. This method enables efficient and regioselective incorporation of isobutane into non-cyclic substrates under mild conditions, followed by intramolecular cyclization to yield indolinone derivatives. Optimal conditions afforded cyclized products in moderate to good yields with high linear selectivity. Substrate scope studies revealed good tolerance, particularly for electron-withdrawing groups. Mechanistic studies using TEMPO as a radical trap showed a 96:4 linear:branched ratio in the C-H activation of isobutane, indicating a highly regioselective HAT pathway. Control experiments using $FeCl_3$ and TBADT as alternative HAT photocatalysts suggest that the active species may originate from a Fe–NFSI complex generating a nitrogen-centered radical *via* ligand-to-metal charge transfer (LMCT). To showcase the method's synthetic utility, a Suzuki cross-coupling reaction was performed, obtaining a derivative with pharmacologically relevant structures such as an indolinone core and a naphthyl group. This is the first reported use of isobutane as an alkylating agent in a photocatalytic cascade cyclization, highlighting the untapped potential of gaseous alkanes in synthetic chemistry.

Resumen

En este trabajo presentamos una ciclación en cascada entre *N*-aril acrilamidas e isobutano basada en una estrategia HAT fotocatalítica. Este método permite la incorporación de isobutano de forma eficiente y regioselectiva a sustratos no cíclicos en condiciones suaves seguida de una ciclación intramolecular para obtener derivados de indolinona. Las condiciones óptimas permiten obtener los productos con rendimientos de moderados a buenos, alta selectividad. El estudio de sustratos reveló buena tolerancia, especialmente con grupos electroatractores. Los estudios mecanísticos utilizando TEMPO como trampa de radicales mostraron una relación de radicales alquilo lineal:ramificada de 96:4, en la activación C-H, lo que indica una vía HAT altamente selectiva. Alternativamente, experimentos de control utilizando $FeCl_3$ y TBADT sugieren que la especie activa podría originarse a partir de un complejo Fe–NFSI que genera un radical centrado en el nitrógeno mediante un proceso LMCT. Para demostrar la utilidad sintética del método, se realizó una reacción de acoplamiento cruzado obteniendo un derivado con estructuras de relevancia farmacológica como un núcleo de indolinona o un grupo naftilo. Este es el primer uso reportado de isobutano como agente alquilante en una ciclación en cascada fotocatalítica, lo que destaca el potencial aún inexplorado de los alcanos gaseosos en la química sintética.

1. Introduction

With a production of 4 trillion m^3 per year, gaseous alkanes represent one of the most abundant yet underutilized carbon-based feedstocks on the planet. In particular, isobutane makes up approximately 0.4% of natural gas and is the smallest alkane with a tertiary carbon. Typically, gaseous alkanes are burned off as fuel or used in processes such as steam cracking or reforming. These processes have raised global concerns from both environmental and economic points of views for being highly energy-intensive and leading to substantial greenhouse gas emissions.[1] As a result, it is highly important to develop protocols which could allow the use of gaseous alkanes as viable alkylating agents in organic synthesis. However, gaseous alkanes are very unreactive due to their low polarity, low solubility in common organic solvents and their high bond dissociation energy[2] (BDE, **Figure 1**). This extreme inertness has rendered their use in organic synthesis very difficult.

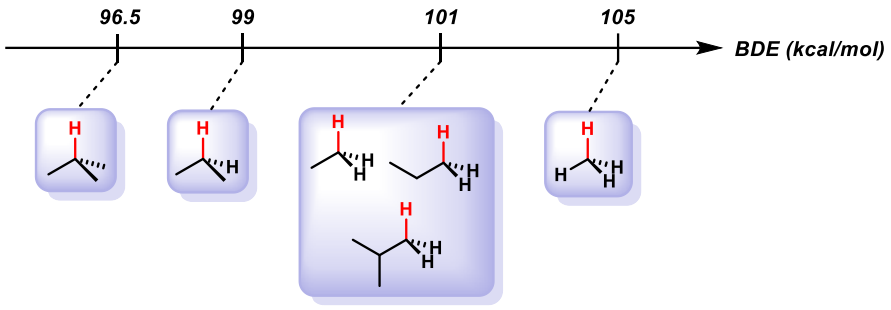

Figure 1. Bond dissociation energies of some gaseous alkanes

In this context, photocatalytic processes based on hydrogen atom transfer (HAT) have become a promising methodology to achieve the direct functionalization of gaseous alkanes.[3,4] Nevertheless, despite the increasing relevance of these approaches, reported precedents of these transformations remain limited.

1.1. Photocatalytic Functionalization of Gaseous Alkanes

In HAT strategy, alkyl radicals are generated from the homolytic cleavage of the C(sp^3)-H bond when exposing the alkane to light and a suitable photocatalyst, allowing its following functionalization.[5] In this process the correlation between the strengths of both the bond being broken and the bond being formed play a crucial role in selectivity and reactivity, and this correlation is considered as the driving force of the reaction. Generally, a decrease in C(sp^3)-H bond strength leads to enhanced rates of the HAT step. Nevertheless, other factors like polar or steric effects can override the preference of HAT for the weakest bonds. In recent years, a variety of photocatalytic systems that allow the functionalization of alkanes in a more selective

and controlled manner have been studied; however, this process remains challenging and underdeveloped.

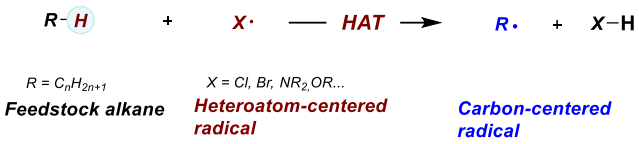

Scheme 1. HAT process

One of the oldest and perhaps the most well-understood tools for photochemical alkane functionalization is the chlorine radical. It is well known that halogen radicals, that are highly electrophilic, can undergo hydrogen atom transfer and generate nucleophilic alkyl radicals. One of the first examples of the utilization of a chlorine radical in alkane functionalization is the discovery of photochlorination of natural gas using Cl_2 by Dumas in 1840,[6] where a chlorine radical abstracts a hydrogen atom from the electron rich C-H bonds of the alkane. Although generating these halogen radicals can be difficult due to the high oxidation potential of H-X or X^-, recent catalytic strategies such as ligand to metal charge transfer (LMCT) have proven to be an interesting and versatile path for generating not only halogen radicals but also other heteroatom-centered radicals.[7] In this process, a metal complex is exposed to light irradiation and an electron is promoted from a filled ligand-based molecular orbital to an empty metal-based molecular orbital[8]. This generates a formally reduced metal center and an oxidized ligand radical, that finally dissociates. For better understanding, the net process can be explained as a homolytic cleavage of the metal-ligand bond (**Figure 2**).

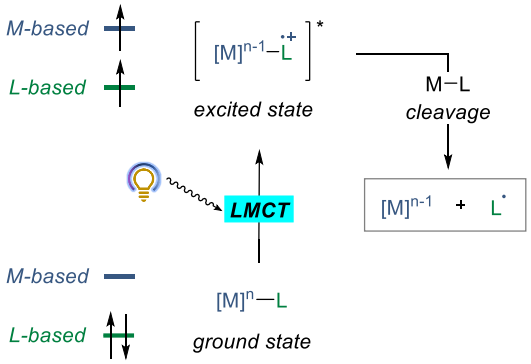

Figure 2. Ligand to Metal Charge Transfer

Although there are few examples of photocatalytic LMCT/HAT functionalization of gaseous alkanes,[9] particularly isobutane remains almost unreported. An example of the functionalization of isobutane *via* HAT/LMCT strategy is a direct alkynylation reported in 2021 by Duan and coworkers[10] (**Scheme 2**).

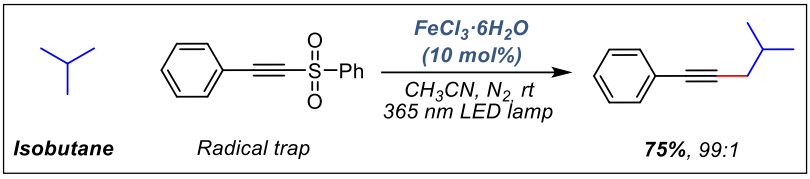

Scheme 2. Direct alkynylation of isobutane

In this study, the authors reported an almost exclusive addition of the linear isobutane radical. As they explain, besides the stability of the radicals (3º>2º>1º) and ratio of chemically inequivalent hydrogens, the steric hindrance in the surroundings of the alkyl radicals played an important role in the regioselectivity observed. In the case of isobutane, despite the tertiary radical being much more stable than the primary one, it also presents a higher steric hindrance that diminishes its addition.

Prof. Timothy Nöel and his group,[11] in 2020, demonstrated a functionalization of gaseous alkanes in flow chemistry using TBADT as photocatalyst. Tetrabutylammonium decatungstate (TBADT) irradiated with light undergoes a HOMO-LUMO transition with LMCT character in which an oxygen-centered radical is generated.[12] This reactive species undergoes HAT with isobutane to generate the corresponding carbon-centered radical that can be trapped by a Michael acceptor to yield the hydroalkylated adduct (**Scheme 3**).

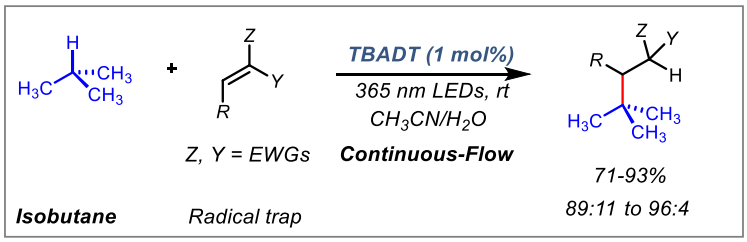

Scheme 3. Isobutane functionalization with TBADT

In 2025, our group reported the cross-coupling of isobutane (and other gaseous alkanes) with (hetero)aryl bromides *via* HAT photocatalysis[13] (**Scheme 4**). The methodology consists of a dual catalytic system composed of TBADT and Ni(II). This system, under the irradiation of a 370 nm LED lamp, afforded the corresponding alkylated products in moderate to good yields.

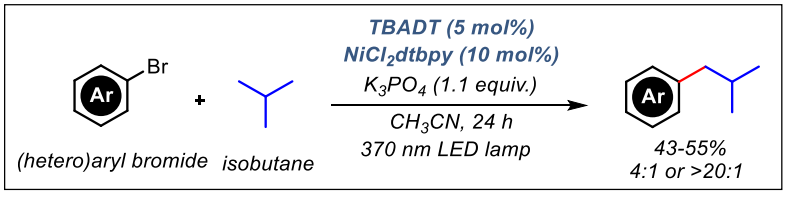

Scheme 4. Cross-coupling of (hetero) aryl bromides with isobutane

The regioselectivity of the reaction varies significantly depending on the nature of the substrate. In the case of aryl bromides, the reaction proceeds with excellent selectivity for the *iso*-butyl product, typically exceeding a 20:1 ratio. In contrast, when heteroaryl bromides are used, the regioselectivity drops to approximately 4:1 in favor of the *iso*-butyl over the *tert*-butyl isomer. The origin of the linear selectivity is attributed to the isomerization of the *tert*-butyl Ni(I) intermediate to the *iso*-butyl Ni(I) intermediate following a *β*-hydride elimination/reinsertion pathway.

Another example of the photoinduced functionalization of isobutane was reported by Gong and coworkers in 2025[14] (**Scheme 5**). In this work, Gong and his team use a dual catalytic system consisting of an organic photocatalyst and a chiral copper catalyst, in combination with different chiral ligands and additives. However, to be able to carry out the transformation, liquified isobutane is added (at -78 ºC). This requirement makes the applicability and scalability of this method very limited.

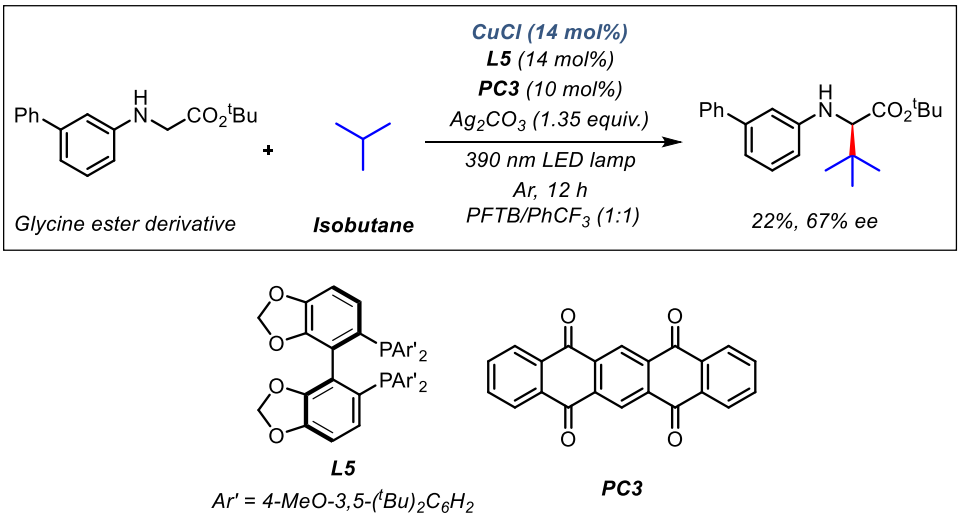

Scheme 5. Photocatalytic alfa alkylation of glycine ester derivatives

While these examples illustrate the utility and advantages of alkane functionalization, the application of these radical processes in cascade cyclizations remain elusive. Particularly, the use of gaseous alkanes in such transformations remain, to our knowledge, unreported.

1.2. Radical Cascade Cyclization

Radical cascade cyclizations offer a particularly attractive strategy for maximizing molecular complexity in an efficient, rapid and atom-economical pathway, in a single step from simple

precursors like isobutane. Typically, to achieve these transformations, prefunctionalized reagents and high temperatures are required. Howerver, there are few examples in which the high reactivity of alkyl radicals generated *via* HAT is utilized to trigger sequential bond-forming events, leading to the rapid construction of cyclic structures. However, current examples of radical cascade cyclizations have only been reported with liquid alkanes.[15]

Indolinone (or oxindole) motifs have been a principal pharmacological building block in the last few years and the central moiety of the structure of various drugs.[16] Radical cyclization *via* thermal initiation is commonly used to synthesize these compounds. In this context, peroxides are frequently employed in C-H activation due to their ability to form oxygen-centered radicals, capable of abstracting hydrogen atoms from electron-rich C(sp^3)-H bonds of alkanes. In 2014, Liu and coworkers[17] reported a copper-mediated alkylarylation of *N*-arylacrylamides with simple alkanes to construct oxindoles with good to excellent yields (**Scheme 6**). In this reaction dicumyl peroxide (DCP) is utilized as the HAT species, and the generation of the oxygen-centered radical is mediated by the copper. Nevertheless, the reaction requires high temperatures to proceed, and the alkane itself must be used as a solvent, which reduces the practical applicability of the reaction.

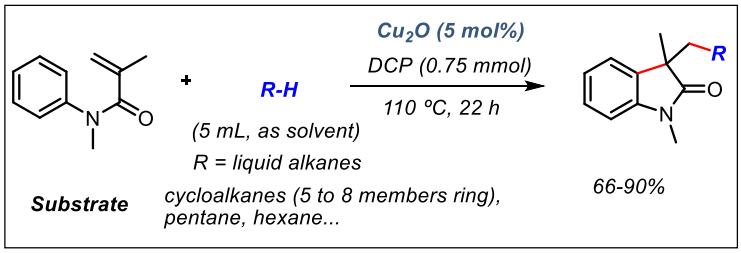

Scheme 6. Copper-mediated synthesis of oxindoles

A different approach involves the photoinduced synthesis of oxindoles using aryl iodides as radical precursors and Cs_2CO_3 as the oxidant.[18] In this method, light irradiation on the aryl iodide produces an aryl radical, which subsequently abstracts a hydrogen atom from the alkane. The reaction operates without a photocatalyst because the aryl iodide is added in stoichiometric amounts. This approach yields the cyclized products containing cycloalkyl groups in 63-68% yields (**Scheme 7**).

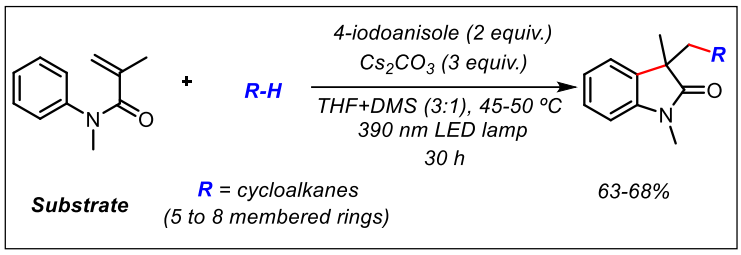

Scheme 7. Photoinduced synthesis of oxindoles

As previously mentioned, TBADT is a well-established catalyst for the C-H activation of simple alkanes. However, due to the inherent challenges of promoting cyclization reactions, only a limited number of studies have employed TBADT in such transformations. In the next example, the synthesis of indolinones was achieved using TBADT as the photocatalyst and $K_2S_2O_8$ as an oxidant,[19] delivering the desired products in moderate to good yields under mild reaction conditions and operational simplicity (**Scheme 8**).

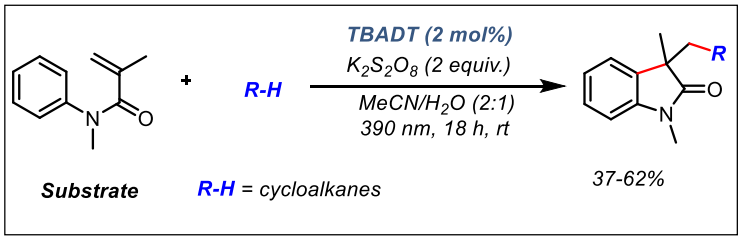

Scheme 8. TBADT catalyzed synthesis of indolinones

Despite these encouraging advances, no examples of radical cascade cyclizations involving gaseous alkanes have been reported to date. This gap underscores a valuable and largely unexplored opportunity in alkane-based synthetic methodology.

2. Objective

Building upon these advances, integrating isobutane radicals into cascade pathways opens new synthetic opportunities for assembling valuable cyclic scaffolds, such as indolinones, under mild and sustainable conditions. Thus, given the experience of the group working with gaseous alkanes we aim to develop a methodology for a cascade cyclization with isobutane through a photocatalytic HAT-based approach.

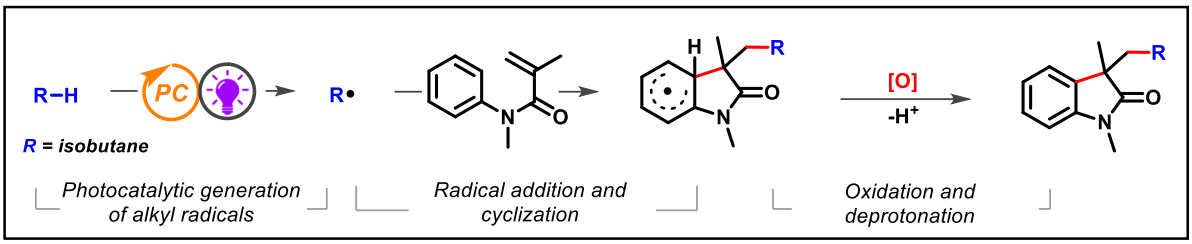

Scheme 9. Objective of the Master's thesis

Therefore, the objectives of this Master's thesis are the following:

- Establish the **optimal conditions** and parameters of the reaction.
- Evaluate the **scope of the reaction** to determine its applicability, potential and limitations.

3. Results and Discussion

3.1. Optimization of the Reaction

We began our optimization by investigating the reaction between *N*-methyl-*N*-phenylmethacrylamide (**1**) and isobutane using a photocatalytic system comprising $FeCl_2$ and N-fluorobenzenesulfonimide (NFSI) (**Table 1**). The initial conditions (10 mol% $FeCl_2$ and 0.4 mmol NFSI in acetonitrile 0.05 M) resulted in minimal product formation and poor conversion (entry 1). Upon the addition of 0.1 mmol LiCl, conversion significantly improved, and 19% yield was obtained, though some activation of the solvent was observed (entry 2). Further dilution of the reaction mixture did not improve the outcome and, in fact, increased solvent activation (entry 3). Increasing the amount of LiCl to 0.2 mmol led to a modest increase in both conversion and yield (entry 4), but the reaction remained unsatisfactory.

Table 1. Optimization of the reaction

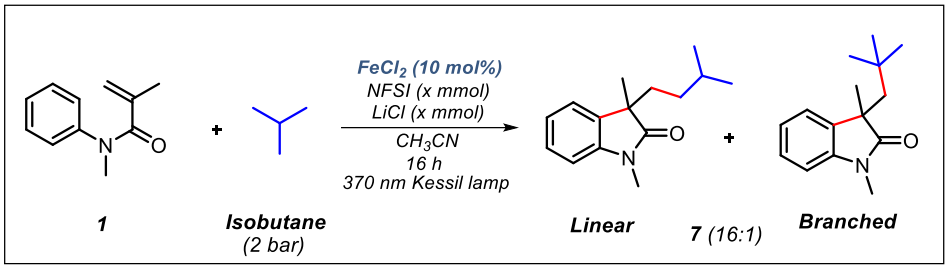

Entry	Conc. (x M)	NFSI (x mmol)	LiCl (x mmol)	Conv. (%)[b]	Yield (%)[a]	AA (%)[b]
1	0.05	0.4	-	35	<10[b]	20*
2	0.05	0.4	0.1	78	19	13*
3	0.025	0.4	0.1	60	18	30
4	0.05	0.4	0.2	83	21	12
5	0.05	0.6	0.2	n.d.	32	34
6[c]	**0.05**	**0.6**	**0.2**	**n.d.**	**63**	**-**
7[d,e]	0.05	-	0.2	n.d.	15	15
8[f]	0.05	0.6	0.2	-	-	-
9[g]	0.05	0.6	0.2	-	-	-
10[h]	0.05	0.6	0.2	n.d.	traces	traces
11[i]	0.05	0.6	0.2	n.d.	25	29
12[j]	0.05	0.6	0.2	n.d.	traces	traces

Reaction conditions: **1** (0.2 mmol), isobutane (2 bar), $FeCl_2$ (10 mol%), NFSI (x mmol), LiCl (x mmol), CH_3CN (x M) at rt for 16 h and irradiation by 370 nm 44W Kessil LED lamp. [a]Yields refer to the isolated product unless otherwise noted. [b]Determined by ^{1}H-NMR using triphenylmethane as internal standard. [c]CD_3CN used as solvent instead of CH_3CN. [d]l:b = 4:1. [e]$K_2S_2O_8$ used instead of NFSI. [f]Reaction performed without $FeCl_2$. [g]Reaction performed in dark. [h]TBADT (10 mol%) instead of $FeCl_2$. [i]$FeCl_3$ (10 mol%) instead of $FeCl_2$. [j]390 or 427 nm instead of 370 nm. Regioselectivity (linear:branched ratio) determined by ^{1}H-NMR analysis. AA=Acetonitrile activation, n.d. = not determined.

An increase in the amount of NFSI to 0.6 mmol led to a marked improvement, establishing the best conditions thus far: 10 mol% $FeCl_2$ as catalyst, 0.6 mmol NFSI as oxidant, and 0.2 mmol LiCl as additive, in acetonitrile (0.05 M), under irradiation with a 44 W 370 nm Kessil LED lamp (entry 5). However, significant acetonitrile activation persisted, prompting a solvent switch to deuterated acetonitrile in order to suppress this side reaction (entry 6). Under these new conditions, we achieved 63% yield, 16:1 regioselectivity favoring linear addition, and no observable solvent activation. As a result, the conditions in entry 6 were selected for subsequent study of the substrate scope.

During the optimization process, we investigated a variety of alternative conditions, including the use of different oxidants and photocatalysts. When potassium persulfate was utilized in place of NFSI (entry 7), the resulting yield was significantly lower than that obtained with NFSI. However, this entry revealed an intriguing aspect regarding regioselectivity. Specifically, the use of potassium persulfate led to a linear-to-branched product ratio of 4:1, which, although still favoring the linear isomer, was considerably lower than the selectivity observed under NFSI conditions. We also evaluated other photocatalysts, such as TBADT and $FeCl_3$. TBADT afforded only trace amounts of product, while $FeCl_3$ gave a reduced yield compared to $FeCl_2$ (entry 10 and 11 respectively). Additionally, a series of control experiments were conducted to assess the necessity of specific reaction components. When the reaction was performed without the iron catalyst (entry 8) or in the absence of light (entry 9), only trace amounts of the desired product were detected, confirming the essential roles of both the photocatalyst and light in enabling the transformation. Furthermore, when the wavelength of the light source was altered to 390 or 427 nm (entry 12), the product yield dropped to just 10%, remaking the importance of the selected 370 nm irradiation for optimal reactivity.

3.2. Scope of the Reaction

After achieving the optimal conditions for the reaction (**Table 1**, entry 6), we decided to move on to the substrate scope. A total of 6 products were synthesized by varying aryl and *N*-substituents affording moderate to good yields and high linear selectivities (**Figure 3**).

Figure 3. Substrate Scope

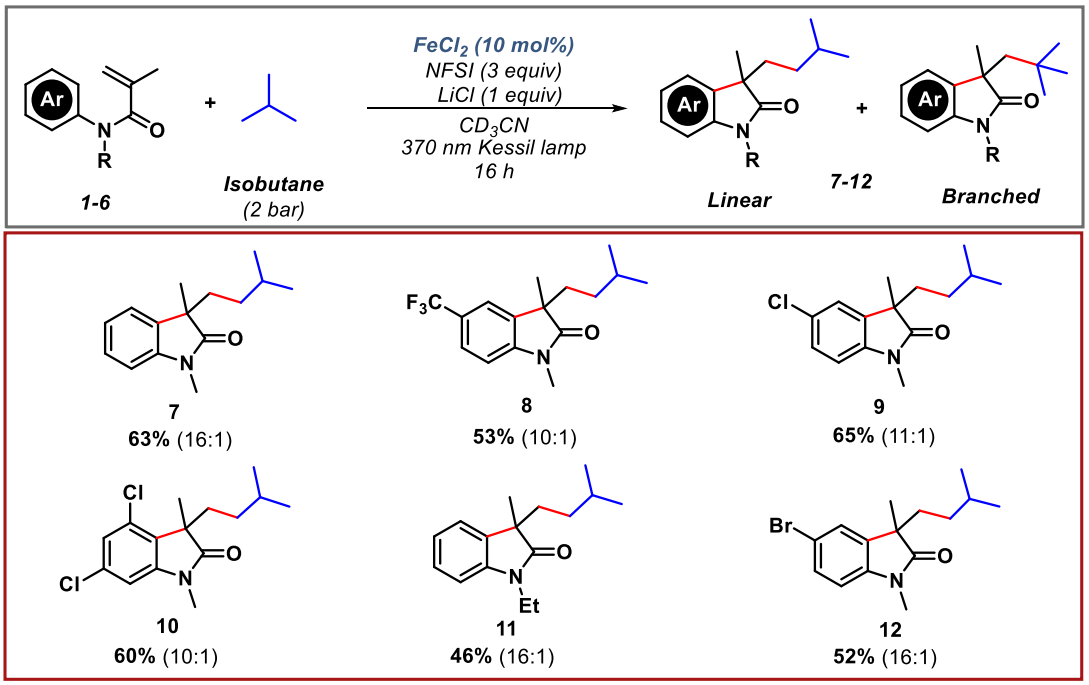

We focused our exploration on substrates containing electron-withdrawing groups (EWGs), including halogens such as chlorine (**9**) and bromine (**12**) at the *para* position, as well as a *para*-substituted trifluoromethyl group (**8**). These modifications afforded the desired products in good yields, likely due to the ability of these EWGs to stabilize the intermediate aryl radical generated during the cyclization step, thereby promoting product formation. In addition, compound **10**, bearing two chlorine substituents at the *meta* positions, was also obtained in good yield, further confirming that electron-withdrawing groups are well tolerated under the reaction conditions and beneficial for the cyclization process. To examine the influence of the nitrogen substituent, we replaced the methyl group with an ethyl group, affording compound **11** in moderate yield. Importantly, all products (**7**-**12**) were isolated with high regioselectivity in favor of the linear isomer determined by ^{1}H-NMR analysis.

3.3. Derivatization Product

Indolinone scaffolds, such as those synthesized in this work, are well-established motifs in drug design[20] and development due to their broad pharmacological activity, especially as anticancer agents. Similarly, terminal alkyl groups are commonly found in a wide range of bioactive molecules with diverse therapeutic applications to enhance their lipophilicity, improving drug absorption. Given that our synthesized compounds incorporate both of these pharmacologically relevant features, we wanted to explore the potential applicability of our methodology in drug discovery by introducing a naphthyl moiety into one of the products, also known to be present in plenty of different drug structures.[21]

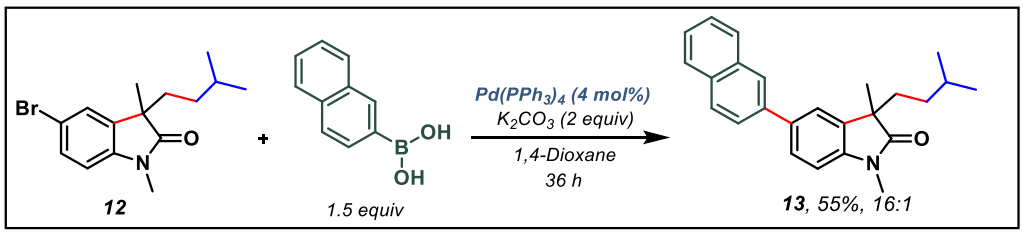

Scheme 10. Suzuki cross-coupling reaction

To this end, compound **12** was selected for a derivatization reaction *via* Suzuki cross-coupling (**Scheme 10**). The resulting compound (**13**) features an indolinone core, a terminal alkyl group, and a naphthyl substituent, combining structural elements frequently encountered in medicinal chemistry.

3.4. Mechanistic Studies

To gain a deeper understanding of how alkyl radicals are generated in this system, we conducted a series of mechanistic experiments using a radical scavenger under various conditions. Firstly, we set up the reaction with the optimized conditions in presence of 2,2,6,6-tetramethylpiperidin-1-oxyl (TEMPO) as the radical scavenger. What we observed was the total suppression of the desired product formation, confirming a radical pathway. Then we planned some experiments to elucidate some key aspects of the radical formation. These experiments were designed to trap and differentiate the two possible alkyl radicals (linear and branched) and to determine their relative ratios (**Table 2**). Accordingly, the reaction was performed without the amide substrate under optimized conditions in the presence of TEMPO. After 16 hours, we successfully detected the TEMPO adducts corresponding to both the linear and branched radicals. Remarkably, the observed ratio was 96:4 in favor of the linear radical (entry 1), which directly aligns with the high linear selectivity noted during the reaction optimization and scope studies. This near-exclusive formation of the linear radical drew our immediate attention, as no other photocatalytic system reported has demonstrated such pronounced regioselectivity in the generation of alkyl radicals from gaseous alkanes. In contrast, the group of Prof. Noël reported that under irradiation with a 365 nm Kessil LED lamp, in flow, TBADT produces isobutane radicals with a regioselectivity of 4:96, heavily favoring the branched radical (entry 2), which is opposite to the selectivity observed in our system. With our reaction setup, in batch, the regioselectivity afforded by TBADT was 11:89 still being favored the branched radical.

Table 2: Alkyl radical trapping with TEMPO

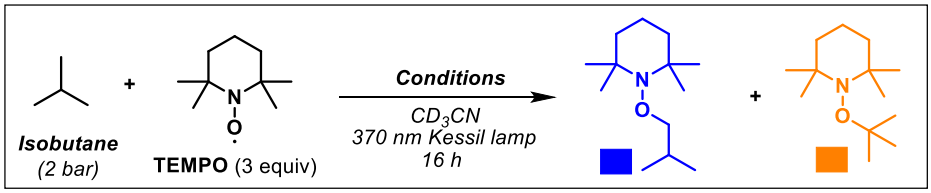

Entry	Conditions	Linear:Branched[a]
1	$FeCl_2$ (10 mol%), NFSI (0.6 mmol), LiCl (0.2 mmol)	96:4
2	TBADT	11:89
3	$FeCl_3$ (10 mol%)	77:23
4	$FeCl_2$ (10 mol%), NFSI (0.6 mmol), no light	Not observed
5	NFSI (0.6 mmol)	Not observed

[a]Ratio determined by GC-MS

To investigate the nature of the species responsible for the HAT process, we repeated the TEMPO trapping experiment using $FeCl_3$ as the catalyst under 370 nm irradiation. The goal was to assess the selectivity profile associated with chlorine radicals and to compare it with that observed under $FeCl_2$/NFSI conditions. This experiment afforded a regioselectivity of 77:23, favoring the linear radical (entry 3). This result is consistent with the known behavior of chlorine radicals, which exhibit minimal preference between abstracting primary or tertiary hydrogens. Given that isobutane contains nine primary hydrogens and only one tertiary hydrogen, this distribution of the two chemically inequivalent hydrogens predominantly explains the observed radical ratio of 77:23.

To further elucidate the mechanism, we performed control experiments to confirm the requirement of specific reaction components for radical generation. When the reaction was carried out in the absence of light (entry 4), no radical trapping products were detected, indicating that photoirradiation is essential for radical formation. Similarly, performing the reaction without $FeCl_2$ (entry 5) also failed to produce any detectable radicals. Together, these results demonstrate that all three components ($FeCl_2$, NFSI, and light) are crucial for initiating the radical process. These findings suggest that the HAT agent in our system is unlikely to be a chlorine radical alone. Instead, it is plausible that there is a competition between chlorine radicals and another, more selective species in the HAT step. Based on the data, we hypothesize that $FeCl_2$ and NFSI may form a reactive complex involving an Fe–N bond. It is well-established that Fe(III) complexes can undergo ligand-to-metal charge transfer (LMCT) processes with halide ligands to generate halogen radicals. Extending this logic, we propose that the Fe–NFSI complex could undergo LMCT to produce a nitrogen-centered radical (**I**), which then engages in HAT with isobutane forming the radical species **II**. Next, **II** adds onto the the alkene of **1** forming the stable α carbonyl radical **III**. This radical undergoes cyclization onto the phenyl ring to form **IV**, which upon oxidation and deprotonation delivers product **7**. The high linear selectivity could be explained due to the high steric hindrance associated with the radical **I**, which may restrict its access to the tertiary C–H bond of isobutane.

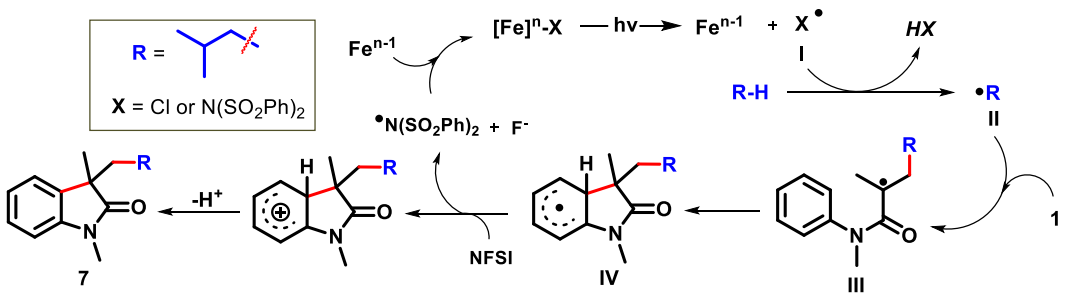

Scheme 11. Plausible mechanism

4. Conclusions

We have developed a photocatalytic HAT-based cascade cyclization of *N*-aryl acrylamides with isobutane, introducing a novel, atom-economical strategy for the efficient and selective incorporation of isobutane into non-cyclic substrates, followed by intramolecular cyclization. This methodology enables the regioselective addition of isobutane gas to a broad range of electron-deficient aryl- and *N*-substituted acrylamides, delivering the corresponding cyclized products under mild and operationally simple conditions.

Mechanistic studies employing TEMPO as a radical scavenger revealed a remarkable 96:4 linear-to-branched ratio in the formation of isobutane-derived radicals, remarking the high regioselectivity of the process. Furthermore, the synthetic utility of the method was demonstrated through the preparation of derivative compound **13** *via* a Suzuki cross-coupling reaction from intermediate **12**, incorporating a naphthyl substituent.

To our knowledge, this represents the first reported protocol for the use of isobutane as an alkylating agent in a cascade cyclization. These findings highlight the broader potential of gaseous alkanes as versatile and underexplored alkylating reagents in synthetic organic chemistry.

5. References

(1) Pulcinella, A.; Mazzarella, D.; Noël, T. Homogeneous Catalytic C(Sp^3)–H Functionalization of Gaseous Alkanes. *Chem. Commun.* **2021**, *57* (78), 9956–9967.

(2) Blanksby, S. J.; Ellison, G. B. Bond Dissociation Energies of Organic Molecules. *Acc. Chem. Res.* **2003**, *36* (4), 255–263.

(3) Ye, Z.; Lin, Y.; Gong, L. The Merger of Photocatalyzed Hydrogen Atom Transfer with Transition Metal Catalysis for C−H Functionalization of Alkanes and Cycloalkanes. *Eur. J. Org. Chem.* **2021**, *2021* (40), 5545–5556.

(4) Velasco-Rubio, Á.; Martínez-Balart, P.; Álvarez-Constantino, A. M.; Fañanás-Mastral, M. C–C Bond Formation *via* Photocatalytic Direct Functionalization of Simple Alkanes. *Chem. Commun.* **2023**, *59* (62), 9424–9444.

(5) Jin, Y.; Zhang, Q.; Wang, L.; Wang, X.; Meng, C.; Duan, C. Convenient C(Sp^3)–H Bond Functionalisation of Light Alkanes and Other Compounds by Iron Photocatalysis. *Green Chem.* **2021**, *23* (18), 6984–6989.

(6) Dumas, J. Ueber das Gesetz der Substitutionen und die Theorie der Typen. *Justus Liebigs Ann. Chem.* **1840**, *33* (3), 259–300.

(7) May, A. M.; Dempsey, J. L. A New Era of LMCT: Leveraging Ligand-to-Metal Charge Transfer Excited States for Photochemical Reactions. *Chem. Sci.* **2024**, *15* (18), 6661–6678.

(8) Juliá, F. Ligand-to-Metal Charge Transfer (LMCT) Photochemistry at 3d-Metal Complexes: An Emerging Tool for Sustainable Organic Synthesis. *ChemCatChem* **2022**, *14* (19), e202200916.

(9) Jin, Y.; Zhang, Q.; Wang, L.; Wang, X.; Meng, C.; Duan, C. Convenient C(Sp^3)–H Bond Functionalisation of Light Alkanes and Other Compounds by Iron Photocatalysis. *Green Chem.* **2021**, *23* (18), 6984–6989.

(10) Jin, Y.; Wang, L.; Zhang, Q.; Zhang, Y.; Liao, Q.; Duan, C. Photo-Induced Direct Alkynylation of Methane and Other Light Alkanes by Iron Catalysis. *Green Chem.* **2021**, *23* (23), 9406–9411.

(11) Laudadio, G.; Deng, Y.; Van Der Wal, K.; Ravelli, D.; Nuño, M.; Fagnoni, M.; Guthrie, D.; Sun, Y.; Noël, T. C(Sp^3)–H Functionalizations of Light Hydrocarbons Using Decatungstate Photocatalysis in Flow. *Science* **2020**, *369* (6499), 92–96.

(12) Ravelli, D.; Fagnoni, M.; Fukuyama, T.; Nishikawa, T.; Ryu, I. Site-Selective C–H Functionalization by Decatungstate Anion Photocatalysis: Synergistic Control by Polar and Steric Effects Expands the Reaction Scope. *ACS Catal.* **2018**, *8* (1), 701–713.

(13) Nair, A. M.; Martínez-Balart, P.; Barbeira-Arán, S.; Fañanás-Mastral, M. Cross-Coupling of Gaseous Alkanes with (Hetero)Aryl Bromides via Dual Nickel/Photoredox Catalysis. *Angew. Chem. Int. Ed.* **2025**, *64* (2), e202416957.

(14) Yang, F.; Chi, L.; Ye, Z.; Gong, L. Photoinduced Regiodivergent and Enantioselective Cross-Coupling of Glycine Derivatives with Hydrocarbon Feedstocks. *J. Am. Chem. Soc.* **2025**, *147* (2), 1767–1780.

(15) Yi, H.; Zhang, G.; Wang, H.; Huang, Z.; Wang, J.; Singh, A. K.; Lei, A. Recent Advances in Radical C–H Activation/Radical Cross-Coupling. *Chem. Rev.* **2017**, *117* (13), 9016–9085.

(16) Koulani, T.; Temizer, A. B.; Karali, N. 2-Indolinone: An Anticancer Scaffold, Overview of the Studies and Approaches (2017–2024). *ChemistrySelect* **2025**, *10* (5), e202405357.

(17) Li, Z.; Zhang, Y.; Zhang, L.; Liu, Z.-Q. Free-Radical Cascade Alkylarylation of Alkenes with Simple Alkanes: Highly Efficient Access to Oxindoles via Selective (Sp^3)C–H and (Sp^2)C–H Bond Functionalization. *Org. Lett.* **2014**, *16* (2), 382–385.

(18) Jha, A. K.; K. L, G.; Yatham, V. R. Photoinduced Cascade Synthesis of Oxindoles and Isoquinolinediones. *J. Org. Chem.* **2025**, *90* (12), 4440–4445.

(19) Fang, X.; Lv, J.; Yang, S.; Ma, M.; Yang, R.; Bi, Y. Cascade C(Sp^3)-H Bond Functionalization/Cyclization Reaction for the Synthesis of 3,3-Disubstituted Oxindoles by Decatungstate Photocatalysis. *Tetrahedron* **2025**, *177*, 134578.

(20) Roy, V. J.; Dagar, N.; Choudhury, S.; Raha Roy, S. Unified Approach to Diverse Heterocyclic Synthesis: Organo-Photocatalyzed Carboacylation of Alkenes and Alkynes from Feedstock Aldehydes and Alcohols. *J. Org. Chem.* **2023**, *88* (21), 15374–15388.

(21) Makar, S.; Saha, T.; Singh, S. K. Naphthalene, a Versatile Platform in Medicinal Chemistry: Sky-High Perspective. *Eur. J. Med. Chem.* **2019**, *161*, 252–276.

6. Annex

6.1. General Experimental Details

6.1.1. Materials and Methods

All reactions were performed under argon atmosphere using oven dried glassware and using standard Schlenk techniques. Solvents were dried using an MBraun SPS 800 system. Isobutane (99.5% purity) was purchased from Nippon Gases. All the amines and other reagents were purchased from AA blocks, Acros Organics B.V.B.A., Aldrich Chemical Co. Ltd., Alfa Aesar, A2B, Apollo, BLD Pharmatech Ltd., Fluorochem Ltd. or TCI Europe N.V. and used without further purification, unless otherwise noted.

The LED light sources used are Kessil PR 160L-370-G2 (max 44 W). Analytical thin layer chromatography was carried out on silica-coated aluminium plates (silica gel 60 F254 Merck) and compounds were visualized using 254 nm UV light. Flash column chromatography was performed using Buchi Pure Chromatography System with FlashPure EcoFlex Silica 4 to 80 g, unless otherwise stated.

GC-MS analyses were performed in an Agilent instrument GC-8890 equipped with Chemical Ionization (CI) MS-5977B detector. High Resolution Mass spectrometry was carried out on a Bruker microTOF spectrometer using APCI-FIA.

^{1}H-, ^{13}C- and ^{19}F-NMR experiments were carried out using a Bruker AVIII-500 MHz or a Varian Mercury 300 MHz or Agilent VNMRS-300 MHz NMR spectrometers. Chemical shift values are reported in ppm with the solvent resonance as the internal standard ($CHCl_3$: δ 7.26 for ^{1}H, δ 77.2 for ^{13}C). Coupling constants (*J*) are given in Hertz (Hz). Multiplicities are reported as follows: s = singlet, d = doublet, t = triplet, q = quartet, p = pentet, hept = heptet, n = nonet, m = multiplet, or as a combination of them.

6.1.2. Reaction Setup

The cyclization reactions (2 bar) were set up using Büchiglasuster tinyclave reactors equipped with steel screw cap with 2 openings 1/8" NPT for: Swagelok® fittings with bursting disc and a manometer valve. Reaction vessel volume was 10 mL with an outer protective mesh. A single LED lamp (Kessil PR 160L-370-G2) was positioned at a distance of 1 cm. A fan was utilized to keep the temperature constant (25 ºC), and the stirring rate was set at 1050 rpm.

6.2. General Procedures

6.2.1. General Procedure for the Synthesis of the Starting Materials (GP1)

N-aryl acrylamides were synthesized in two steps from the corresponding aryl amine and methacrylic acid. Both reagents were purchased from Aldrich Chemical Co. Ltd. The first coupling reaction was performed following the procedure described by Zhao and coworkers[I]. In the second step, the *N*-methylation was performed following the protocol described by Li[II].

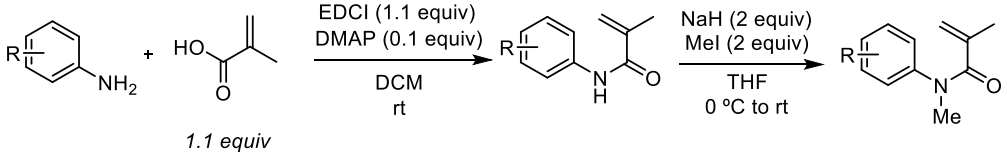

To a 100 mL round bottom flask equipped with a stirring bar were added primary amines (1 equiv, 10 mmol), DMAP (0.1 equiv, 1 mmol), EDCI (1.1 equiv, 11 mmol), methacrylic acid (1.1 equiv, 11 mmol) and DCM (50 mL). The reaction was stirred at room temperature overnight (16 h). After completion of the reaction the solvent was removed under reduced pressure to obtain the crude product, the pure amide was obtained by silica gel chromatography.

To a solution of the amide (1 equiv, 6 mmol) in THF (50 mL) was added in portions NaH (2 equiv, 12 mmol) at 0 ºC. After stirring for 15 min at the same temperature MeI (2 equiv, 12

[I] Zhao, X.; Li, W.; Zhou, L.; Zhao, X.; Zhang, Y.; Li, B.; Li, R.; Zhu, L. Cu(II)-Catalyzed Hydroboration Reactions of 1,1-Disubstituted α,β-Unsaturated Ketones, Esters, and Amides in Pure Water. *J. Org. Chem.,* **2024**, 89, 8334–8341.

[II] Li, Y. L.; Wang, J. B.; Wang, X. L.; Cao, Y.; Deng, J. Silver-Catalyzed Decarboxylative Radical Addition/Cyclization of α,α-Difluoroarylacetic Acids with Acrylamides To Synthesize Difluorinated Oxindoles. *Eur. J. Org. Chem.,* **2017**, 2017, 6052–6059.

mmol) was added. The mixture was warmed to rt and stirred for 5 h. The reaction was quenched with H_2O and the aqueous layer was extracted three times with EtOAc. The combined organic layers were dried over Na_2SO_4, filtered and concentrated under reduced pressure. The crude product was purified by silica gel chromatography to obtain product correspondent *N*-aryl acrylamide.

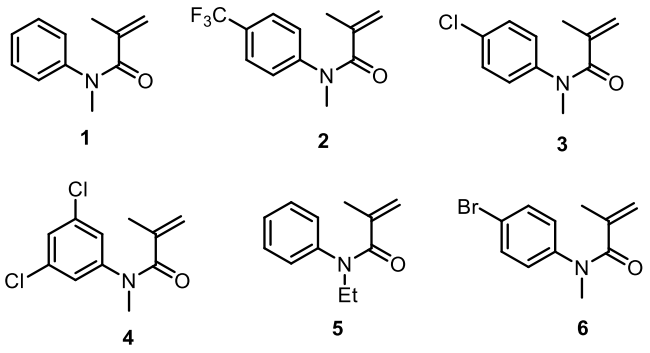

Compounds **1** to **6** have been previously characterized, and the spectroscopic data were in accordance with the reported literature[III]. Compound **5** was synthesized using EtI instead of MeI.

6.2.2. General Procedure for the Cyclization Reactions with Isobutane (GP2)

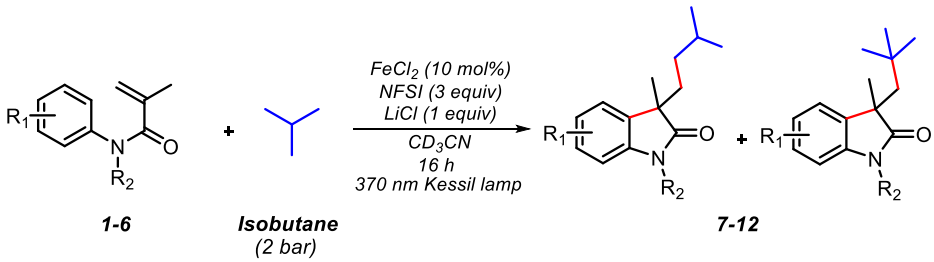

In a reaction vessel equipped with a stirring bar a solution of $FeCl_2$ (10 mol%, 0.02 mmol), NFSI (3 equiv, 0.6 mmol), LiCl (1 equiv, 0.2 mmol), *N*-aryl acrylamide (1 equiv, 0.2 mmol) in CD_3CN (4 mL) was added. The reactor was closed and 5 cycles of vacuum followed by 2 bar

[III] (a) Li, Y. L.; Wang, J. B.; Wang, X. L.; Cao, Y.; Deng, J. Silver-Catalyzed Decarboxylative Radical Addition/Cyclization of α,α-Difluoroarylacetic Acids with Acrylamides To Synthesize Difluorinated Oxindoles. *Eur. J. Org. Chem.,* **2017**, 2017, 6052–6059. (b) Matcha, K., Narayan, R., & Antonchick, A. P. Metal-Free Radical Azidoarylation of Alkenes: Rapid Access to Oxindoles by Cascade C-N and C-C Bond-Forming Reactions. *Angew. Chem. Int. Ed.*, **2013**, 52, 7985–7989.

of isobutane were performed. After the last cycle the reaction was kept at 2 bar of isobutane for 10 min. Then, the valve of the reactor was closed, and the reaction was stirred under irradiation of 370 nm Kessil lamp for 16 h with a fan pointed to the reactor to keep the temperature constant (rt). The reaction was transferred to a round bottom flask and the solvent was removed in vacuo. The residue was purified by silica gel chromatography.

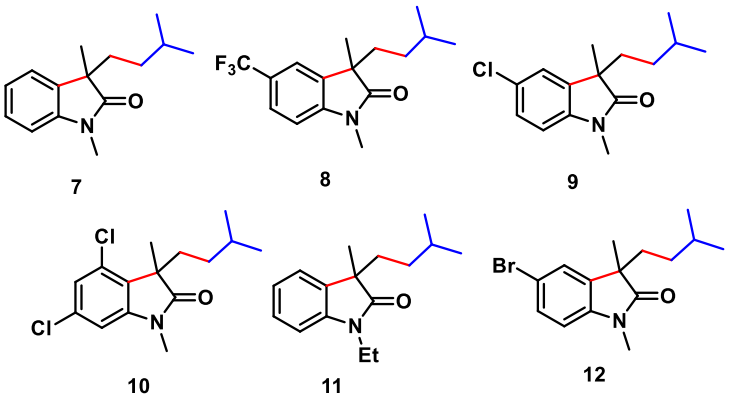

6.2.3. General Procedure for the Derivatization Product (GP3)

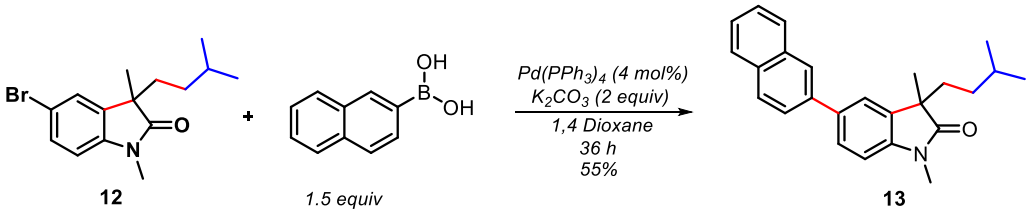

In a Schlenk tube equipped with a stirring bar, K_2CO_3 (2 equiv, 0.2 mmol), 2-Naphtaleneboronic acid (1.5 equiv, 0.15 mmol) and $Pd(PPh_3)_4$ (4 mol%) were added. Then 1 mL of a solution of 5-bromo-3-isopentyl-1,3-dimethylindolin-2-one (**12**) (1 equiv, 0.1 mmol) in 1,4-Dioxane was added. The reaction mixture was heated to 80 ºC and stirred for 36 h. The reaction was quenched with water, extracted three times with EtOAc, filtered and concentrated under reduced pressure. The residue was purified by silica gel chromatography to obtain product **13** in 55% yield.

6.3. Characterization of the Products

3-isopentyl-1,3-dimethylindolin-2-one (7)

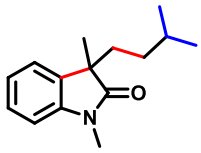

Synthesized from *N*-methyl-*N*-phenylmethacrylamide (**1**) and isobutane following GP2. Obtained in 63% yield after flash column chromatography (Hexane/AcOEt 9:1). The r.r. 16:1 was determined by ^{1}H-NMR. Characterization is only given for the major regioisomer.

^{1}H NMR (500 MHz, $CDCl_3$) δ 7.28 (t, *J* = 7.1 Hz, 1H), 7.18 (d, *J* = 7.4 Hz, 1H), 7.08 (t, *J* = 7.4 Hz, 1H), 6.86 (d, *J* = 7.7 Hz, 1H), 3.23 (s, 3H), 1.90 (td, *J* = 12.9, 4.7 Hz, 1H), 1.75 (td, *J* = 13.1, 4.3 Hz, 1H), 1.42 (dq, *J* = 13.3, 6.7 Hz, 1H), 1.37 (s, 3H), 0.95 – 0.86 (m, 1H), 0.79 (dd, *J* = 8.7, 6.7 Hz, 6H), 0.75 – 0.65 (m, 1H). **^{13}C NMR** (126 MHz, $CDCl_3$) δ 180.9, 143.4, 134.3, 127.6, 122.4, 122.4, 107.9, 48.3, 36.4, 33.2, 28.2, 26.1, 23.9, 22.5, 22.3. **HRMS (APCI)**: Calc. for $C_{15}H_{22}NO$ [M+H$^+$] 232.1696, found 232.1697.

3-isopentyl-1,3-dimethyl-5-(trifluoromethyl)indolin-2-one (8)

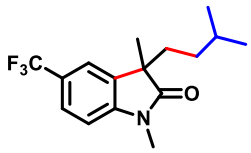

Synthesized from *N*-methyl-*N*-(4-(trifluoromethyl)phenyl)methacrylamide (**2**) and isobutane following GP2. Obtained in 53% yield after flash column chromatography (Hexane/AcOEt 10:1). The r.r. 10:1 was determined by ^{1}H-NMR. Characterization is only given for the major regioisomer.

^{1}H NMR (500 MHz, $CDCl_3$) δ 7.55 (d, *J* = 8.1 Hz, 1H), 7.38 (d, *J* = 1.8 Hz, 1H), 6.90 (d, *J* = 8.1 Hz, 1H), 3.24 (s, 3H), 1.92 (td, *J* = 13.0, 4.6 Hz, 1H), 1.75 (td, *J* = 13.1, 4.2 Hz, 1H), 1.46 – 1.37 (m, 1H), 1.37 (s, 3H), 0.86 (tdd, *J* = 12.8, 6.6, 4.5 Hz, 1H), 0.78 (dd, *J* = 9.1, 6.6 Hz, 6H), 0.67 (tdd, *J* = 12.8, 6.8, 4.3 Hz, 1H). **^{13}C NMR** (126 MHz, $CDCl_3$) δ 179.3, 140.9, 135.1, 126.8, 126.5, 122.0, 107.8, 47.7, 35.3, 32.1, 27.1, 25.2, 22.8, 21.4, 21.3. *Quaternary C heterocoupled with F could not be seen. **^{19}F NMR** (282 MHz, $CDCl_3$) δ -68.0. **HRMS (APCI)**: Calc. for $C_{16}H_{21}F_3NO$ [M+H$^+$] 300.1570, found 300.1567.

5-chloro-3-isopentyl-1,3-dimethylindolin-2-one (9)

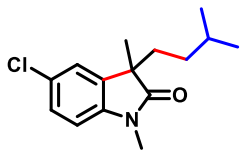

Synthesized from *N*-(4-chlorophenyl)-*N*-methylmethacrylamide (**3**) and isobutane following GP2. Obtained in 65% yield after flash column chromatography (Hexane/AcOEt 9:1). The r.r. 11:1 was determined by ^{1}H-NMR. Characterization is only given for the major regioisomer.

^{1}H NMR (500 MHz, $CDCl_3$) δ 7.23 (dd, *J* = 8.2, 2.1 Hz, 1H), 7.12 (d, *J* = 2.1 Hz, 1H), 6.75 (d, *J* = 8.2 Hz, 1H), 3.19 (s, 3H), 1.88 (td, *J* = 13.0, 4.5 Hz, 1H), 1.69 (td, *J* = 13.0, 4.2 Hz, 1H), 1.40 (hept, *J* = 6.8 Hz, 1H), 1.33 (s, 3H), 0.88 – 0.80 (m, 1H), 0.78 (dd, *J* = 7.3, 6.6 Hz, 6H), 0.73 – 0.64 (m, 1H). **^{13}C NMR** (126 MHz, $CDCl_3$) δ 179.3, 140.9, 135.1, 126.8, 126.5, 122.0, 107.8, 47.7, 35.3, 32.1, 27.1, 25.2, 22.8, 21.4, 21.3. **HRMS (APCI)**: Calc. for $C_{15}H_{21}ClNO$ [M+H$^+$] 266.1306, found 266.1298.

4,6-dichloro-3-isopentyl-1,3-dimethylindolin-2-one (10)

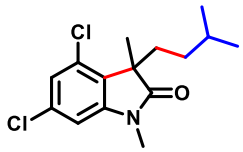

Synthesized from *N*-(3,5-dichlorophenyl)-*N*-methylmethacrylamide (**4**) and isobutane following GP2. Obtained in 60% yield after flash column chromatography (Hexane/AcOEt 9:1). The r.r. 10:1 was determined by ^{1}H-NMR. Characterization is only given for the major regioisomer.

^{1}H NMR (500 MHz, $CDCl_3$) δ 7.01 (d, *J* = 1.7 Hz, 1H), 6.74 (d, *J* = 1.7 Hz, 1H), 3.19 (s, 3H), 2.22 (td, *J* = 13.1, 4.3 Hz, 1H), 1.89 (td, *J* = 13.0, 4.5 Hz, 1H), 1.46 (s, 3H), 1.47 – 1.38 (m, 1H), 0.78 (d, *J* = 6.6 Hz, 6H), 0.77 – 0.69 (m, 1H), 0.61 – 0.50 (m, 1H). **^{13}C NMR** (126 MHz, $CDCl_3$) δ 179.1, 144.9, 133.1, 129.8, 127.4, 122.0, 106.3, 49.1, 32.7, 32.3, 27.0, 25.4, 21.6, 21.1, 20.6. **HRMS (APCI)**: Calc. for $C_{15}H_{20}Cl_2NO$ [M+H$^+$] 300.0916, found 300.0909.

1-ethyl-3-isopentyl-3-methylindolin-2-one (11)

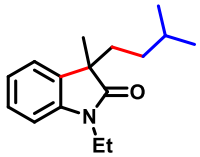

Synthesized from *N*-ethyl-*N*-phenylmethacrylamide (**5**) and isobutane following GP2. Obtained in 46% yield after flash column chromatography (Hexane/AcOEt 9:1). The r.r. 16:1 was determined by ^{1}H-NMR. Characterization is only given for the major regioisomer.

^{1}H NMR (500 MHz, $CDCl_3$) δ 7.25 (td, *J* = 7.7, 1.3 Hz, 1H), 7.16 (dd, 1H), 7.05 (td, *J* = 7.5, 0.9 Hz, 1H), 6.85 (d, *J* = 7.8 Hz, 1H), 3.77 (dheptd, *J* = 51.8, 14.3, 7.2 Hz, 2H), 1.88 (td, *J* = 12.8, 4.6 Hz, 1H), 1.72 (td, *J* = 12.9, 4.2 Hz, 1H), 1.39 (hept, *J* = 13.3, 6.7 Hz, 1H), 1.34 (s, 3H), 1.25 (t, *J* = 7.2 Hz, 3H), 0.97 – 0.83 (m, 1H), 0.77 (dd, *J* = 7.7, 6.7 Hz, 6H), 0.71 – 0.65 (m, 1H). **^{13}C NMR** (126 MHz, $CDCl_3$) δ 180.6, 142.6, 134.7, 127.6, 122.8, 122.3, 108.1, 48.3, 36.5, 34.6, 33.3, 28.3, 24.0, 22.6, 22.4, 12.9. **HRMS (APCI)**: Calc. for $C_{16}H_{24}NO$ [M+H$^+$] 246.1852, found 246.1847.

5-bromo-3-isopentyl-1,3-dimethylindolin-2-one (12)

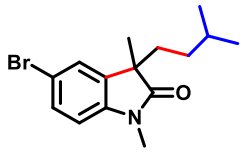

Synthesized from *N*-(4-bromophenyl)-*N*-methylmethacrylamide (**6**) and isobutane following GP2. Obtained in 52% yield after flash column chromatography (Hexane/AcOEt 9:1). The r.r. 16:1 was determined by ^{1}H-NMR. Characterization is only given for the major regioisomer.

^{1}H NMR (500 MHz, $CDCl_3$) δ 7.38 (dd, *J* = 8.1, 1.7 Hz, 1H), 7.26 (d, *J* = 1.9 Hz, 1H), 6.71 (d, *J* = 8.2 Hz, 1H), 3.19 (s, 3H), 1.88 (td, *J* = 12.9, 4.5 Hz, 1H), 1.69 (td, *J* = 13.0, 4.3 Hz, 1H), 1.44 – 1.37 (m, 1H), 1.33 (s, 3H), 0.88 – 0.81 (m, 1H), 0.78 (t, *J* = 7.0 Hz, 6H), 0.73 – 0.65 (m, 1H). **^{13}C NMR** (126 MHz, $CDCl_3$) δ 179.2, 141.4, 135.5, 129.4, 124.7, 114.2, 108.3, 47.6, 35.3, 32.1, 27.1, 25.2, 22.8, 21.4, 21.3. **HRMS (APCI)**: Calc. for $C_{15}H_{21}BrNO$ [M+H$^+$] 310.0801, found 310.0806.

3-isopentyl-1,3-dimethyl-5-(naphthalen-2-yl)indolin-2-one (13)

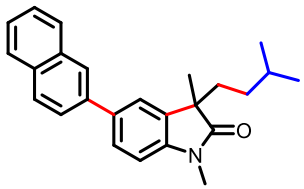

Synthesized from 5-bromo-3-isopentyl-1,3-dimethylindolin-2-one (**12**) and isobutane following GP3. Obtained in 55% yield after flash column chromatography (Hexane/AcOEt 9:1). The r.r. 16:1 was determined by ^{1}H-NMR. Characterization is only given for the major regioisomer.

^{1}H NMR (500 MHz, $CDCl_3$) δ 8.01 (d, 1H), 7.90 (dd, 3H), 7.73 (dd, *J* = 8.5, 1.9 Hz, 1H), 7.64 (dd, *J* = 8.0, 1.8 Hz, 1H), 7.53 – 7.46 (m, 3H), 6.95 (d, *J* = 8.0 Hz, 1H), 3.28 (s, 3H), 1.96 (td, *J* = 12.9, 4.6 Hz, 1H), 1.82 (td, *J* = 13.0, 4.2 Hz, 1H), 1.44 (s, 3H), 1.48 – 1.40 (m, 1H), 0.98 – 0.90 (m, 1H), 0.80 (dd, *J* = 9.6, 6.6 Hz, 6H), 0.83 – 0.75 (m, 1H). **^{13}C NMR** (126 MHz, $CDCl_3$) δ 141.9, 137.5, 134.8, 134.1, 132.7, 131.4, 127.5, 127.0, 126.7, 125.8, 125.4, 124.8, 124.5, 124.2, 120.6, 107.2, 47.6, 35.5, 32.2, 27.2, 25.3, 23.0, 21.5, 21.3. **HRMS (APCI)**: Calc. for $C_{25}H_{27}NO$ [M+H$^+$] 358.2170, found 358.2158.

6.4. NMR Spectra of the Products (7-13)

Note: ✸ Signal at 0.61 (^{1}H)/30 (^{13}C) ppm corresponds to 9H of the *tert*-butyl group in the minor branched regiosiomer.

3-isopentyl-1,3-dimethylindolin-2-one (7)

^{1}H NMR (500 MHz, $CDCl_3$)

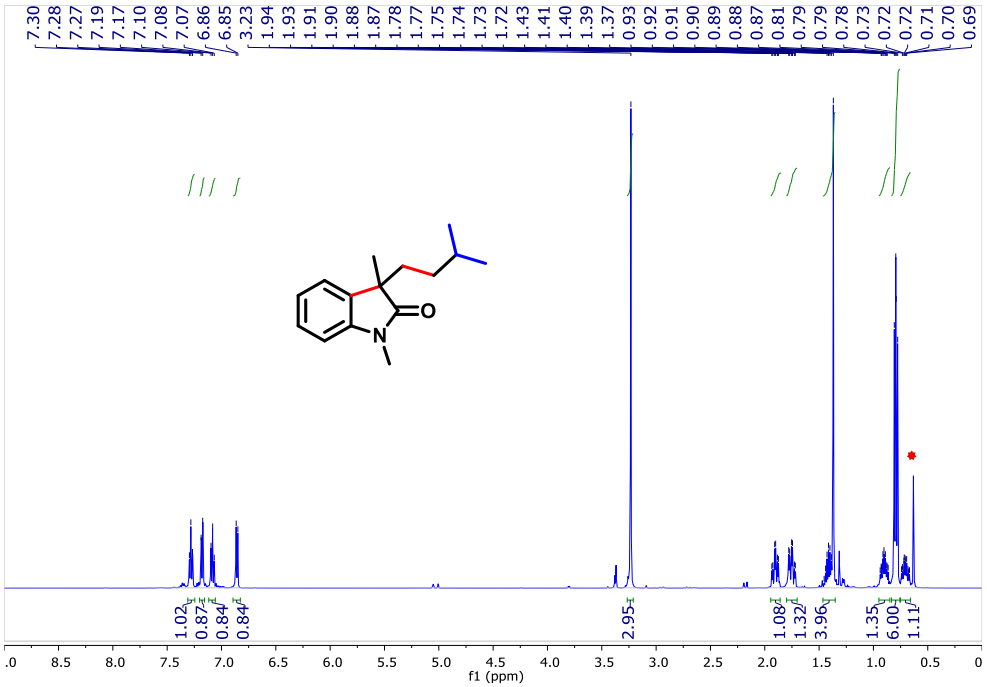

^{13}C NMR (126 MHz, $CDCl_3$)

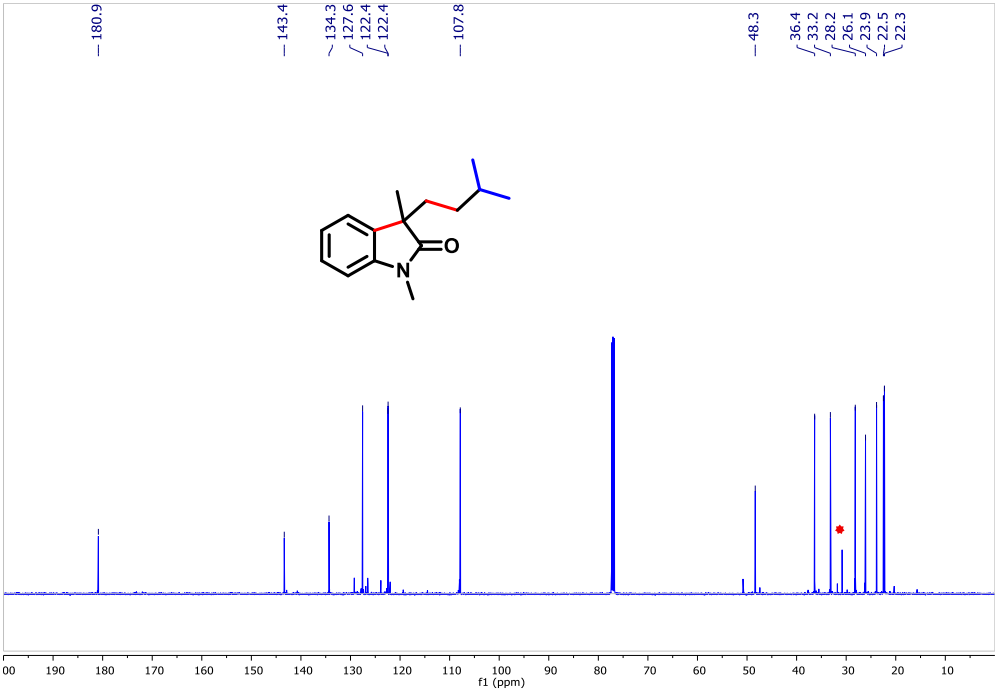

3-isopentyl-1,3-dimethyl-5-(trifluoromethyl)indolin-2-one (8)

^{1}H NMR (500 MHz, $CDCl_3$)

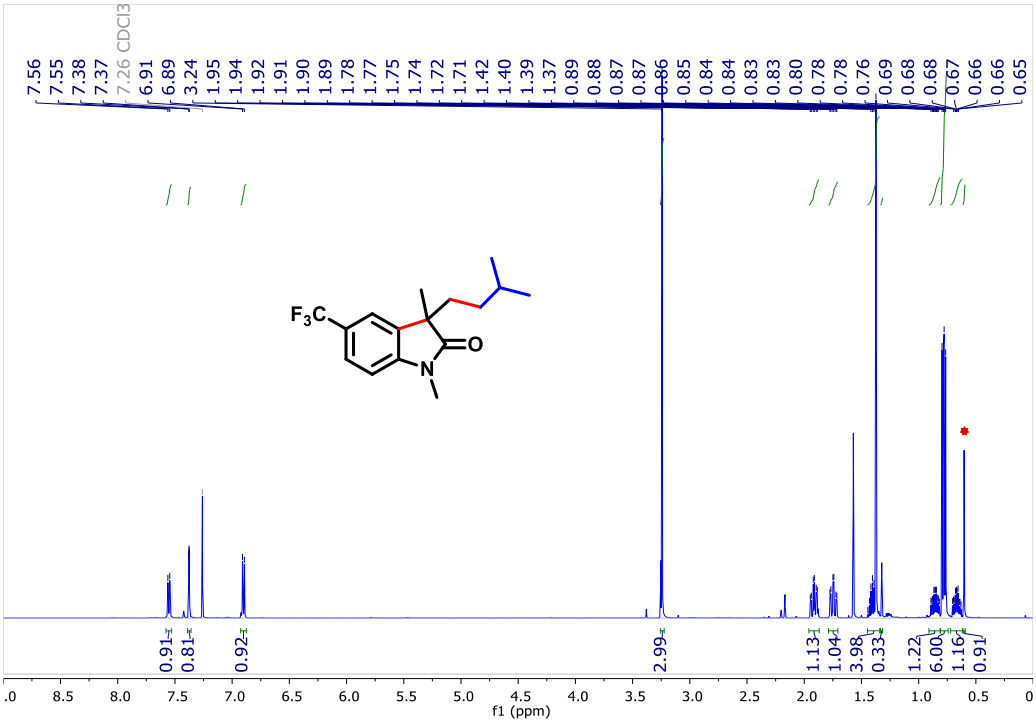

^{13}C NMR (126 MHz, $CDCl_3$)

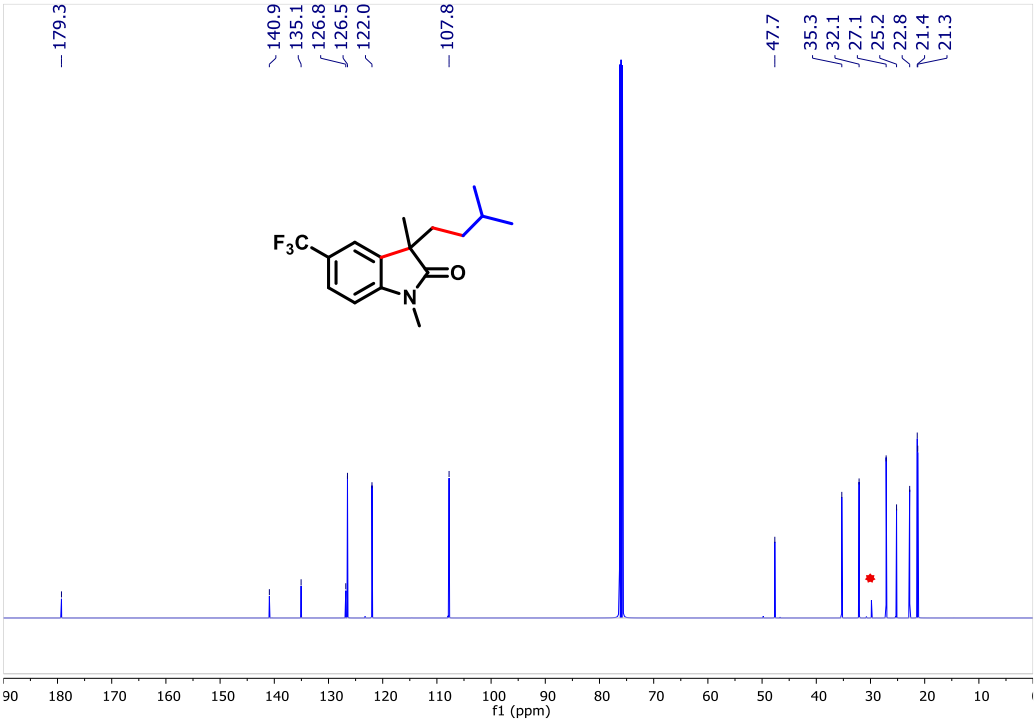

^{19}F NMR (282 MHz, $CDCl_3$)

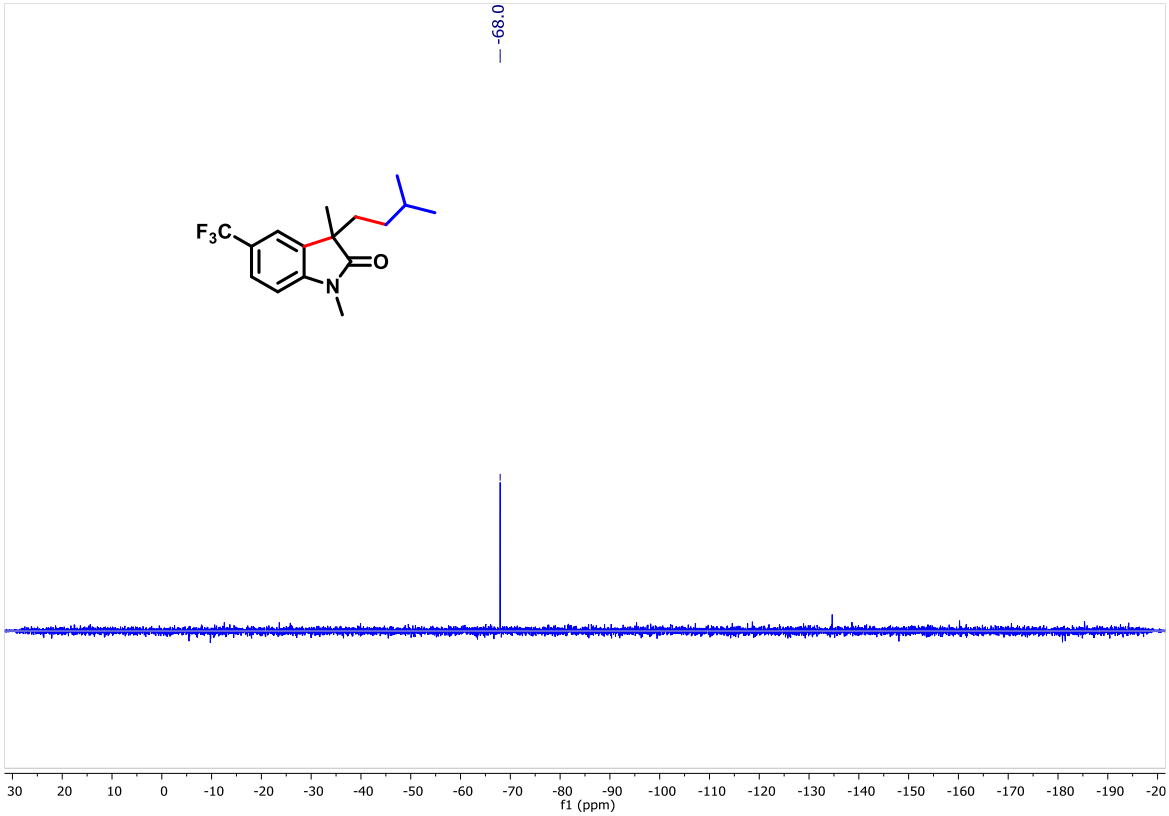

5-chloro-3-isopentyl-1,3-dimethylindolin-2-one (9)

^{1}H NMR (500 MHz, $CDCl_3$)

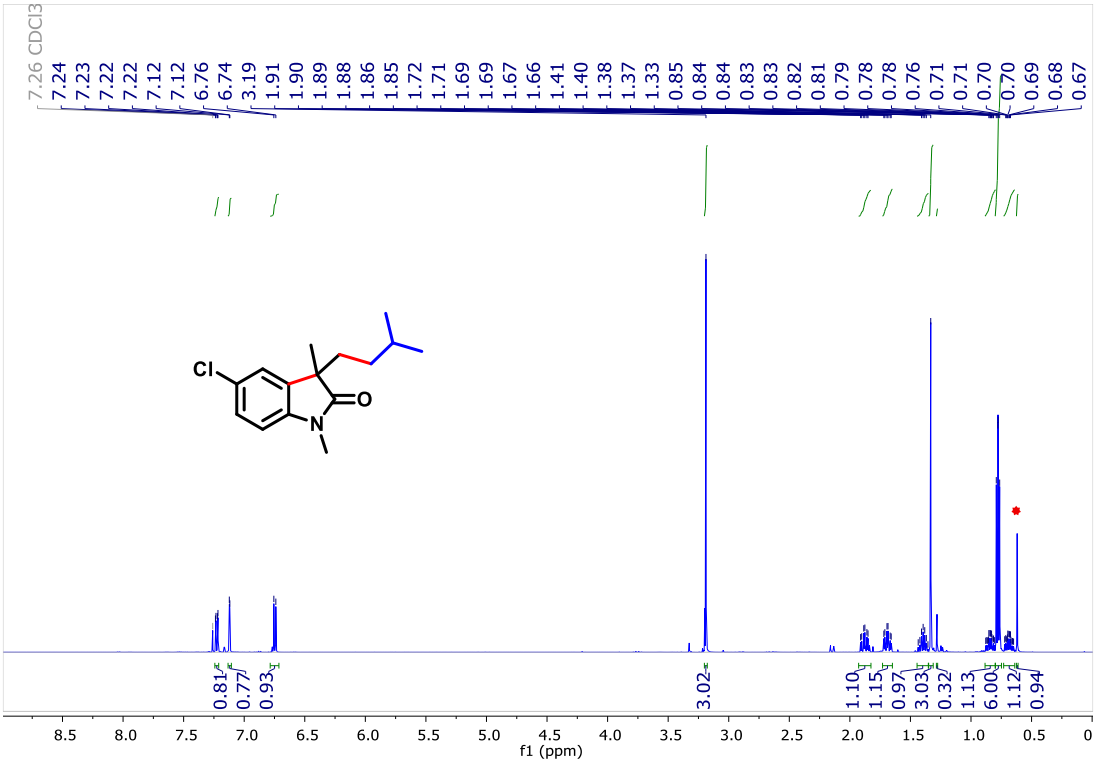

^{13}C NMR (126 MHz, $CDCl_3$)

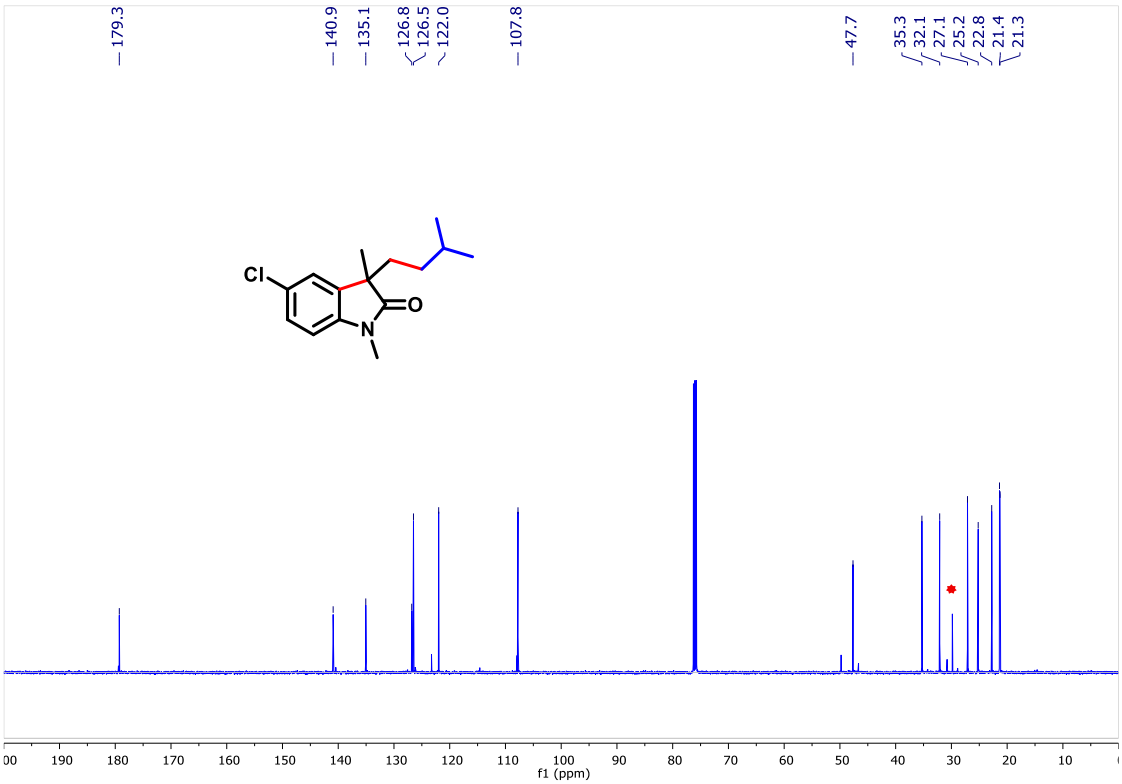

4,6-dichloro-3-isopentyl-1,3-dimethylindolin-2-one (10)

^{1}H NMR (500 MHz, $CDCl_3$)

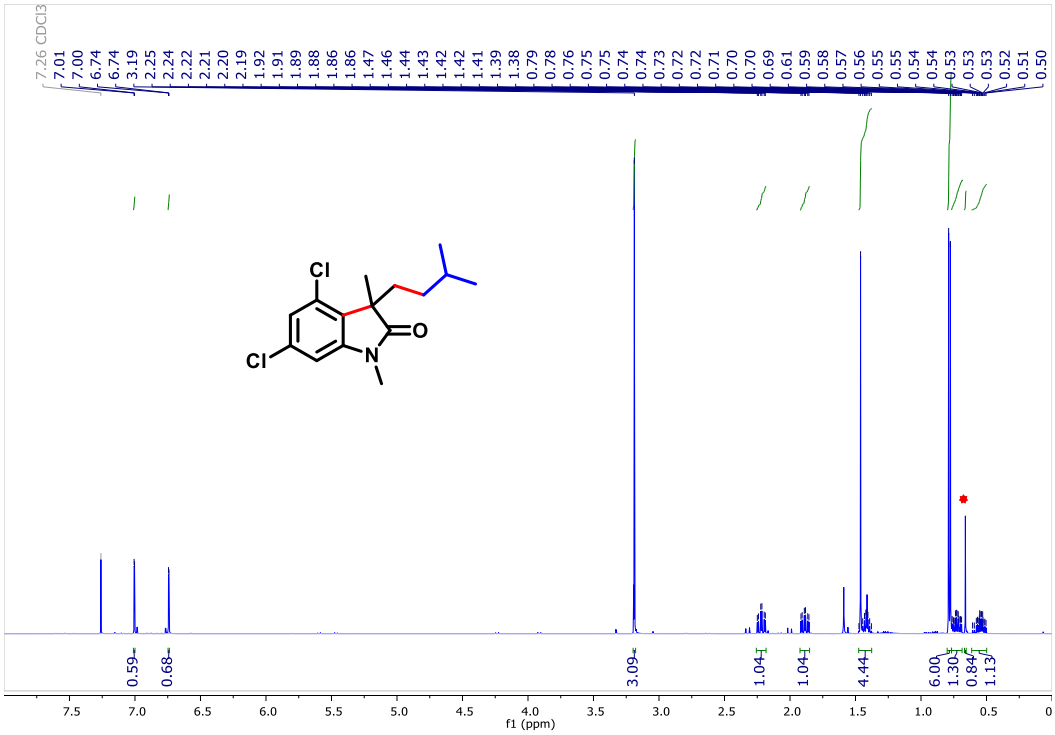

^{13}C NMR (126 MHz, $CDCl_3$)

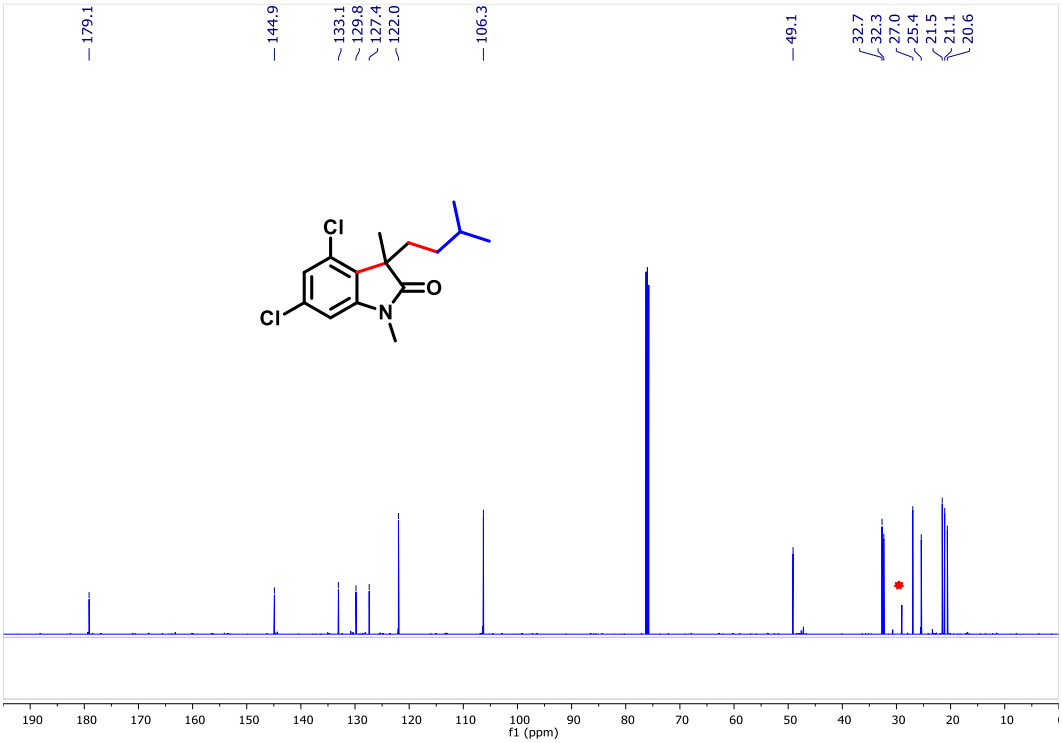

1-ethyl-3-isopentyl-3-methylindolin-2-one (11)

^{1}H NMR (500 MHz, $CDCl_3$)

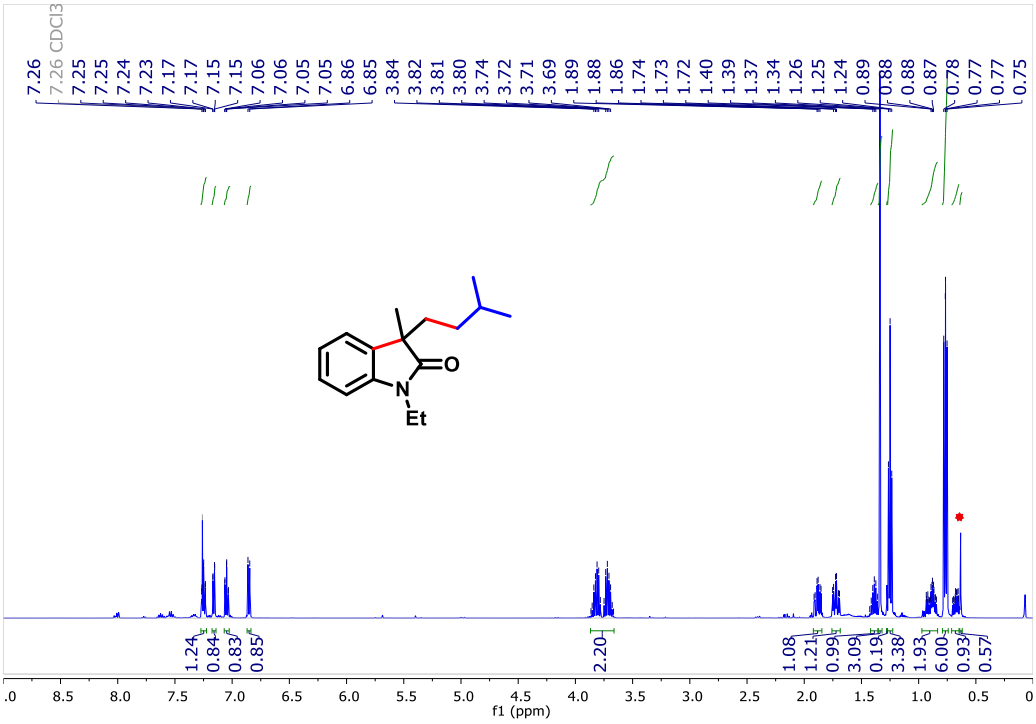

^{13}C NMR (126 MHz, $CDCl_3$)

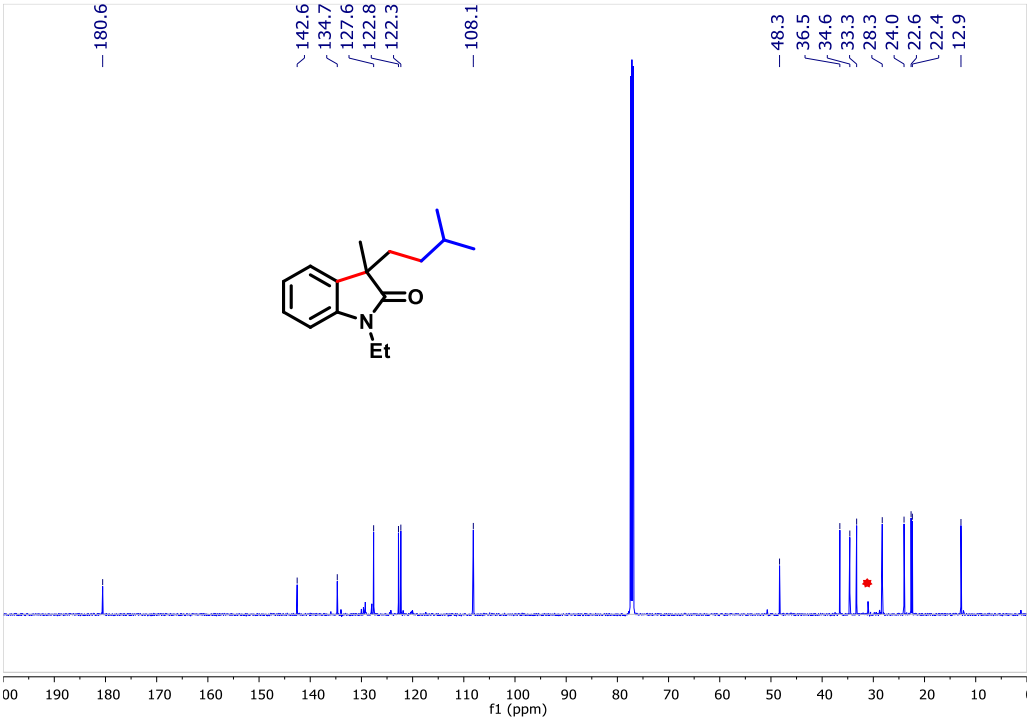

5-bromo-3-isopentyl-1,3-dimethylindolin-2-one (12)

^{1}H NMR (500 MHz, $CDCl_3$)

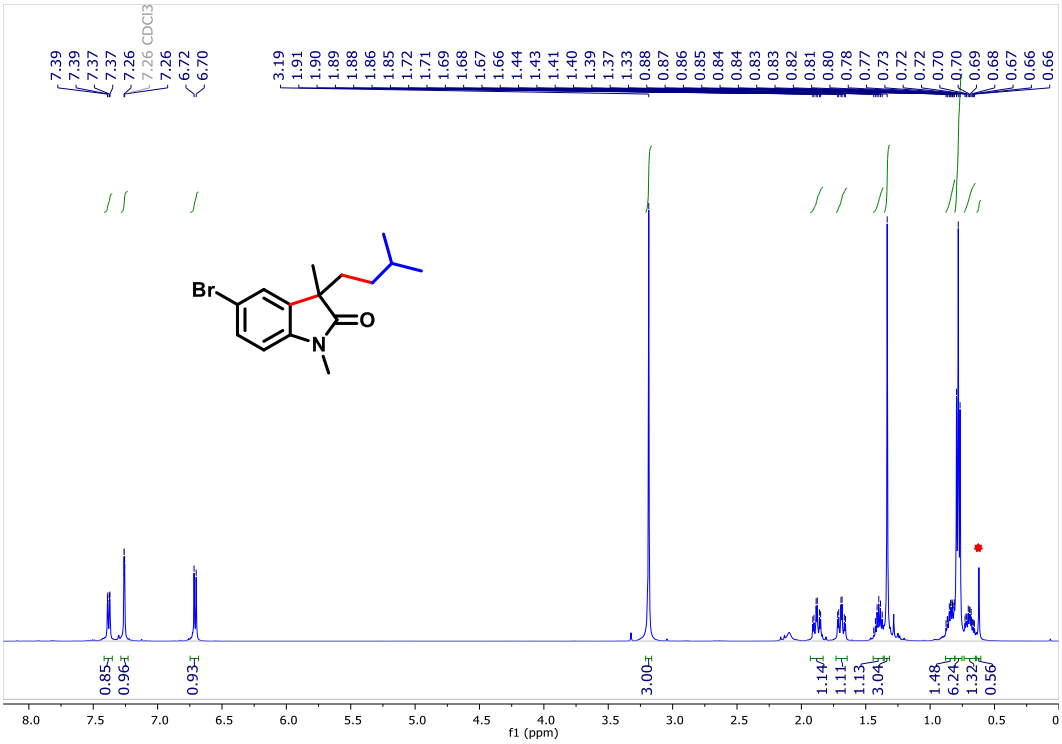

^{13}C NMR (126 MHz, $CDCl_3$)

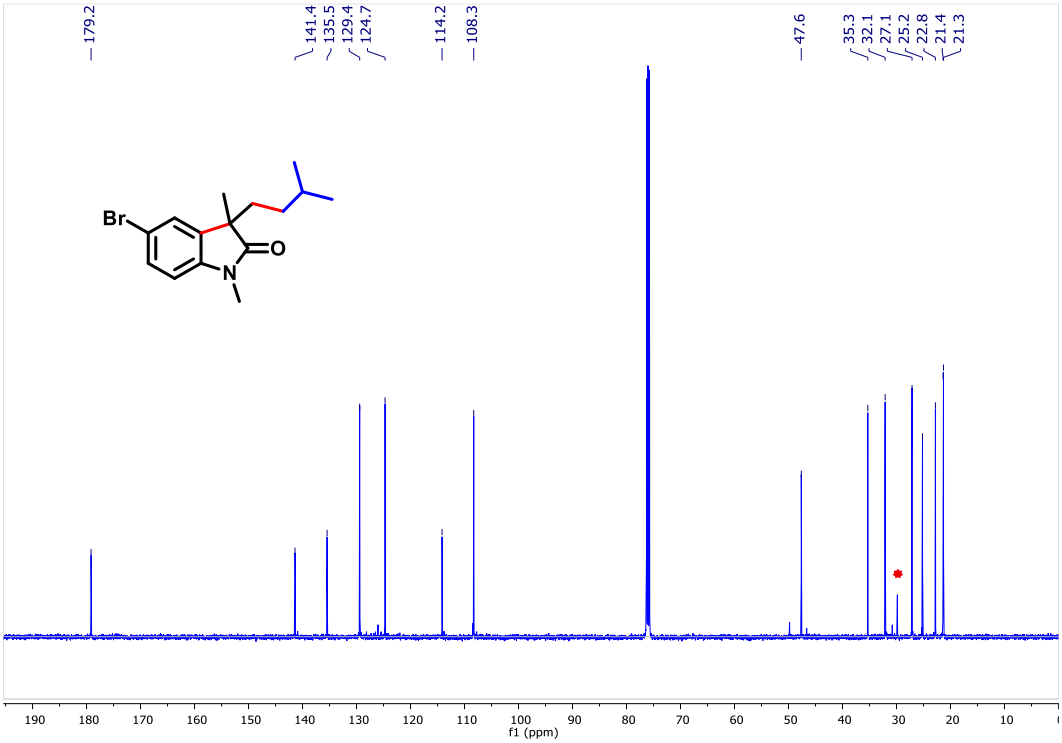

3-isopentyl-1,3-dimethyl-5-(naphthalen-2-yl)indolin-2-one (13)

^{1}H NMR (500 MHz, $CDCl_3$)

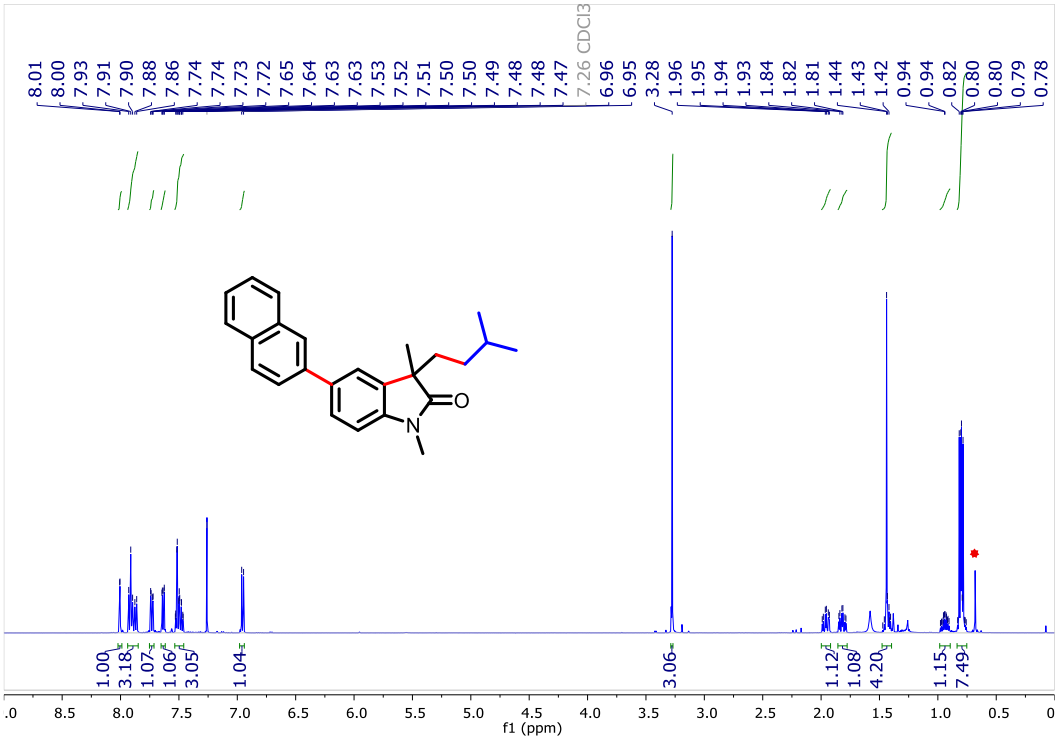

^{13}C NMR (126 MHz, $CDCl_3$)